The Astrophysical Journal Letters, 829:L4 (7pp), 2016 September 20 doi:10.3847/2041-8205/829/1/L4

DISCOVERY OF A SUBSTELLAR COMPANION TO THE NEARBY DEBRIS DISK HOST HR 2562

Quinn M. Konopacky[1], Julien Rameau[2], Gaspard Duchêne[3,4], Joseph C. Filippazzo[5], Paige A. Giorla Godfrey[6,7,8], Christian Marois[9,10], Eric L. Nielsen[11,12], Laurent Pueyo[5], Roman R. Rafikov[13], Emily L. Rice[6,7,8], Jason J. Wang[3], S. Mark Ammons[14], Vanessa P. Bailey[12], Travis S. Barman[15], Joanna Bulger[16], Sebastian Bruzzone[17], Jeffrey K. Chilcote[18], Tara Cotten[19], Rebekah I. Dawson[20], Robert J. De Rosa[3], René Doyon[2], Thomas M. Esposito[3], Michael P. Fitzgerald[21], Katherine B. Follette[12], Stephen Goodsell[22,23], James R. Graham[3], Alexandra Z. Greenbaum[24], Pascale Hibon[25], Li-Wei Hung[21], Patrick Ingraham[26], Paul Kalas[3], David Lafrenière[2], James E. Larkin[21], Bruce A. Macintosh[12], Jérôme Maire[18], Franck Marchis[11], Mark S. Marley[27], Brenda C. Matthews[9,10], Stanimir Metchev[17,28], Maxwell A. Millar-Blanchaer[18,29], Rebecca Oppenheimer[8], David W. Palmer[14], Jenny Patience[30], Marshall D. Perrin[5], Lisa A. Poyneer[14], Abhijith Rajan[30], Fredrik T. Rantakyrö[23], Dmitry Savransky[31], Adam C. Schneider[32], Anand Sivaramakrishnan[5], Inseok Song[19], Remi Soummer[5], Sandrine Thomas[26], J. Kent Wallace[33], Kimberly Ward-Duong[30], Sloane J. Wiktorowicz[34], and Schuyler G. Wolff[24]

[1] Center for Astrophysics and Space Sciences, University of California, San Diego, La Jolla, CA 92093, USA; qkonopacky@ucsd.edu
[2] Institut de Recherche sur les Exoplanètes, Département de physique, Université de Montréal, Montréal, QC H3C 3J7, Canada
[3] Astronomy Department, University of California, Berkeley, Berkeley, CA 94720, USA
[4] Univ. Grenoble Alpes/CNRS, IPAG, F-38000 Grenoble, France
[5] Space Telescope Science Institute, Baltimore, MD 21218, USA
[6] Department of Engineering Science and Physics, College of Staten Island, City University of New York, Staten Island, NY 10314, USA
[7] Physics Program, The Graduate Center, City University of New York, New York, NY 10016, USA
[8] Department of Astrophysics, American Museum of Natural History, New York, NY 10024, USA
[9] National Research Council of Canada Herzberg, Victoria, BC V9E 2E7, Canada
[10] University of Victoria, Department of Physics and Astronomy, 3800 Finnerty Road, Victoria, BC V8P 5C2, Canada
[11] SETI Institute, Carl Sagan Center, Mountain View, CA 94043, USA
[12] Kavli Institute for Particle Astrophysics and Cosmology, Department of Physics, Stanford University, Stanford, CA 94305, USA
[13] Institute for Advanced Study, Princeton, NJ 08540, USA
[14] Lawrence Livermore National Laboratory, 7000 East Avenue, Livermore, CA, 94550, USA
[15] Lunar and Planetary Lab, University of Arizona, Tucson, AZ 85721, USA
[16] Subaru Telescope, NAOJ, 650 North Aohoku Place, Hilo, HI 96720, USA
[17] Department of Physics and Astronomy, Centre for Planetary Science and Exploration, The University of Western Ontario, London, ON N6A 3K7, Canada
[18] Dunlap Institute for Astronomy & Astrophysics, University of Toronto, 50 St. George Street, Toronto, ON, Canada
[19] Department of Physics and Astronomy, University of Georgia, Athens, GA 30602, USA
[20] Center for Exoplanets and Habitable Worlds, The Pennsylvania State University, 525 Davey Laboratory, University Park, PA, 16802, USA
[21] Department of Physics & Astronomy, University of California, Los Angeles, CA 90095, USA
[22] Department of Physics, Durham University, Stockton Road, Durham DH1, UK
[23] Gemini Observatory, Casilla 603, La Serena, Chile
[24] Department of Physics & Astronomy, Johns Hopkins University, Baltimore MD 21218, USA
[25] European Southern Observatory, Alonso de Cordova 3107, Vitacura, Santiago, Chile
[26] Large Synoptic Survey Telescope, 950 N Cherry Avenue, Tucson AZ, 85719, USA
[27] Space Science Division, NASA Ames Research Center, Mail Stop 245-3, Moffett Field CA 94035, USA
[28] Department of Physics & Astronomy, Stony Brook University, Stony Brook, NY 11794-3800, USA
[29] Department of Astronomy & Astrophysics, University of Toronto, 50 St. George Street, Toronto, ON, Canada
[30] School of Earth and Space Exploration, Arizona State University, P.O. Box 871404, Tempe, AZ 85287, USA
[31] Sibley School of Mechanical and Aerospace Engineering, Cornell University, Ithaca, NY 14853, USA
[32] Department of Physics & Astronomy, University of Toledo, 2801 W. Bancroft Street, Toledo, OH 43606, USA
[33] Jet Propulsion Laboratory, California Institute of Technology, 4800 Oak Grove Drive, Pasadena, CA 91109, USA
[34] The Aerospace Corporation, 2310 E. El Segundo Boulevard, El Segundo, CA 90245,USA
Received 2016 July 7; revised 2016 August 11; accepted 2016 August 22; published 2016 September 14

ABSTRACT

We present the discovery of a brown dwarf companion to the debris disk host star HR 2562. This object, discovered with the Gemini Planet Imager (GPI), has a projected separation of 20.3 ± 0.3 au (0.″618 ± 0.″004) from the star. With the high astrometric precision afforded by GPI, we have confirmed, to more than 5σ, the common proper motion of HR 2562B with the star, with only a month-long time baseline between observations. Spectral data in the *J*-, *H*-, and *K*-bands show a morphological similarity to L/T transition objects. We assign a spectral type of L7 ± 3 to HR 2562B and derive a luminosity of $\log(L_{\rm bol}/L_{\odot}) = -4.62 \pm 0.12$, corresponding to a mass of 30 ± 15 $M_{\rm Jup}$ from evolutionary models at an estimated age of the system of 300–900 Myr. Although the uncertainty in the age of the host star is significant, the spectra and photometry exhibit several indications of youth for HR 2562B. The source has a position angle that is consistent with an orbit in the same plane as the debris disk recently resolved with *Herschel*. Additionally, it appears to be interior to the debris disk. Though the extent of the inner hole is currently too uncertain to place limits on the mass of HR 2562B, future observations of the disk with higher spatial resolution may be able to provide mass constraints. This is the first brown-dwarf-mass object found to reside in the inner hole of a debris disk, offering the opportunity to search for evidence of formation above the deuterium burning limit in a circumstellar disk.

Key words: brown dwarfs – instrumentation: adaptive optics – planet–disk interactions – stars: individual (HR 2562)

Supporting material: data behind figure

1. INTRODUCTION

There is considerable interest in determining whether Jovian planets on wide orbits represent a continuum that extends to brown dwarf masses or whether there is a strong cutoff in the number of companions as a function of mass (e.g., Kratter et al. 2010). This relates to possible formation pathways for substellar companions: either companions form within a circumstellar disk and reach a mass above the deuterium burning limit (e.g., Vorobyov 2013) or via cloud fragmentation, as in binary systems with a high mass ratio (q; Bate 2012). Population statistics from direct imaging provide essential observational parameters for testing formation history. From numerous surveys, only a handful of imaged substellar companions are $<$100 au from their host stars. In particular, this separation regime has shown a lack of brown dwarfs with $q < 0.1$ (the "brown dwarf desert"; e.g., Kraus et al. 2008) around stars with $M > 0.5 M_{\odot}$. However, this parameter space has recently begun to be populated by direct imaging (e.g., Hinkley et al. 2015; Mawet et al. 2015).

Since the contrast of a substellar object is more favorable for imaging with youth, direct imaging surveys tend to target sources with evidence of a relatively young age ($<$300 Myr). The presence of a debris disk, leftover from planet formation, is a clue for a younger-than-field age, since the dust luminosity is known to decrease with time (see Wyatt 2008). However, the dust can persist for longer times if small planetesimals are dynamically perturbed by an orbiting companion, hence other youth indicators are necessary to constrain the age of a star. An accurate estimate of the age of the star is necessary since companion properties are often derived from evolutionary models. Membership in nearby young associations (e.g., Malo et al. 2013) provides the tightest constraints on the age of a star; otherwise, large variation in the derived companion masses exists (e.g., Kuzuhara et al. 2013; Fuhrmann & Chini 2015).

Among the brown dwarf-mass companions that have been discovered around stars with infrared excess, none have been previously seen inside the inner hole of a resolved disk, which offers the opportunity to study dynamical interactions. Using the Gemini Planet Imager (GPI; Macintosh et al. 2014), we report the discovery of a companion to the debris disk host HR 2562. HR 2562B has a projected separation within the "brown dwarf desert," and within a possible cleared inner hole. We derive properties for this companion based on spectra and colors, and discuss the potential role it plays in maintaining and shaping the debris disk.

2. HR 2562

HR 2562 is a F5V star with an estimated mass of 1.3 $M_{\odot}$ (Gray et al. 2006; Casagrande et al. 2011). It has a distance of 33.63 ± 0.48 pc and a proper motion of $\sim$110 mas yr^{-1} (van Leeuwen 2007). It was identified as having a debris disk with data from *IRAS* and *Spitzer* by Moór et al. (2006). Gray et al. (2006) identify the source as active based on the Ca II H and K lines, while Torres et al. (2000) identify it as an X-ray source. Several groups have also computed metallicity estimates, which range from [M/H] = [−0.05, +0.08] (Gray et al. 2006; Casagrande et al. 2011; Maldonado et al. 2012), with possible evidence of peculiar individual abundances (Casagrande et al. 2011).

Currently there are several disparate age estimates for HR 2562 in the literature. An estimate of 300 ± 120 Myr was made by Asiain et al. (1999), who used a combination of space motions and evolutionary model-derived ages to suggest that the source is part of a nearby Local Association subgroup called B3. In their identification of the source using *IRAS*, Rhee et al. (2007) use space motions, a lithium non-detection, and X-ray luminosity to give a rough age estimate of $\sim$300 Myr. Conversely, analysis of data from the Geneva–Copenhagen survey, in which metallicities and temperatures were used to derive ages from models, gives an estimated age of 0.9–1.6 Gyr (Casagrande et al. 2011). In their assessment of age based on Ca II H and K lines, Pace (2013) also derived an age of $\sim$900 Myr. Most recently, Moór et al. (2015) used photometric modeling with atmosphere models to derive an age range of 300^{+420}_{-180} Myr. The BANYAN II group/field membership estimation code (Gagné et al. 2014) gives low probabilities for the star as belonging to any known young nearby group, but suggests the star is younger than field stars, giving a wide range of possible ages between $\sim$20 Myr and $\sim$1 Gyr. While the age of the star remains uncertain, sufficient evidence of moderate youth led to the inclusion of HR 2562 in the sample for the Gemini Planet Imager Exoplanet Survey (GPIES). For the purposes of this paper, we adopt a nominal age range of 300–900 Myr.

3. GPI OBSERVATIONS AND DATA ANALYSIS

HR 2562 was observed in 2016 January. GPIES observations are taken in the angular differential imaging (ADI; Marois et al. 2006) H-band spectroscopic mode. A candidate companion was identified in this initial data set. Follow-up observations were made within a month in the $K1$-, $K2$-, and J-bands. Sky frames were also obtained right after the $K2$ sequence. Table 1 gives the log of these observations. Weather conditions were median, with DIMM seeing around 1″ when available. Another (longer) $K2$ sequence was acquired to provide higher a signal-to-noise ratio for the companion and was used for spectroscopy. All data were acquired with the H-band apodizer providing a near-IR constant star-to-satellite-spot[35] ratio of 9.23 ± 0.06 mag (Perrin et al. 2016). Astrometric calibrator observations were obtained in 2016 January and February, and were analyzed following Konopacky et al. (2014). These observations showed no change in the IFS calibration as measured in previous GPIES observations. Therefore, following De Rosa et al. (2015), a pixel scale and a position angle offset of 14.166 ± 0.007 mas/px and -0.10 ± 0.13 deg were used.

Data were processed using the GPI data reduction pipeline version 1.3.0 (Perrin et al. 2016 and the references therein) to obtain calibrated (x, y, λ) datacubes. Further processing to suppress the star point-spread function was performed as

[35] Satellite spots are diffraction spots created by a square grid placed in the pupil plane.

Table 1
Observations and Astrometry of HR 2562B

Date (UT)	Filter	$\lambda/\delta\lambda$	Total Int. Time (minutes)	Field Rot. (deg)	ρ (mas)	θ (deg)	Contrast (mag)	Absolute Mag.
2016 Jan 25	*H*	45	37	20.2	619 ± 3	297.56 ± 0.35	11.7 ± 0.1	14.2 ± 0.1
2016 Jan 28	*K*1	65	23	11.9	618 ± 5	297.40 ± 0.25	10.6 ± 0.1	13.0 ± 0.1
2016 Jan 28	*K*2	75	24	11.3	618 ± 4	297.76 ± 0.37	10.4 ± 0.1	12.8 ± 0.1
2016 Feb 25	*K*2	75	47	25.7	619 ± 2	297.50 ± 0.25	10.4 ± 0.1	12.8 ± 0.1
2016 Feb 28	*J*	35	54	26.6	620 ± 3	297.90 ± 0.25	12.6 ± 0.1	15.3 ± 0.1

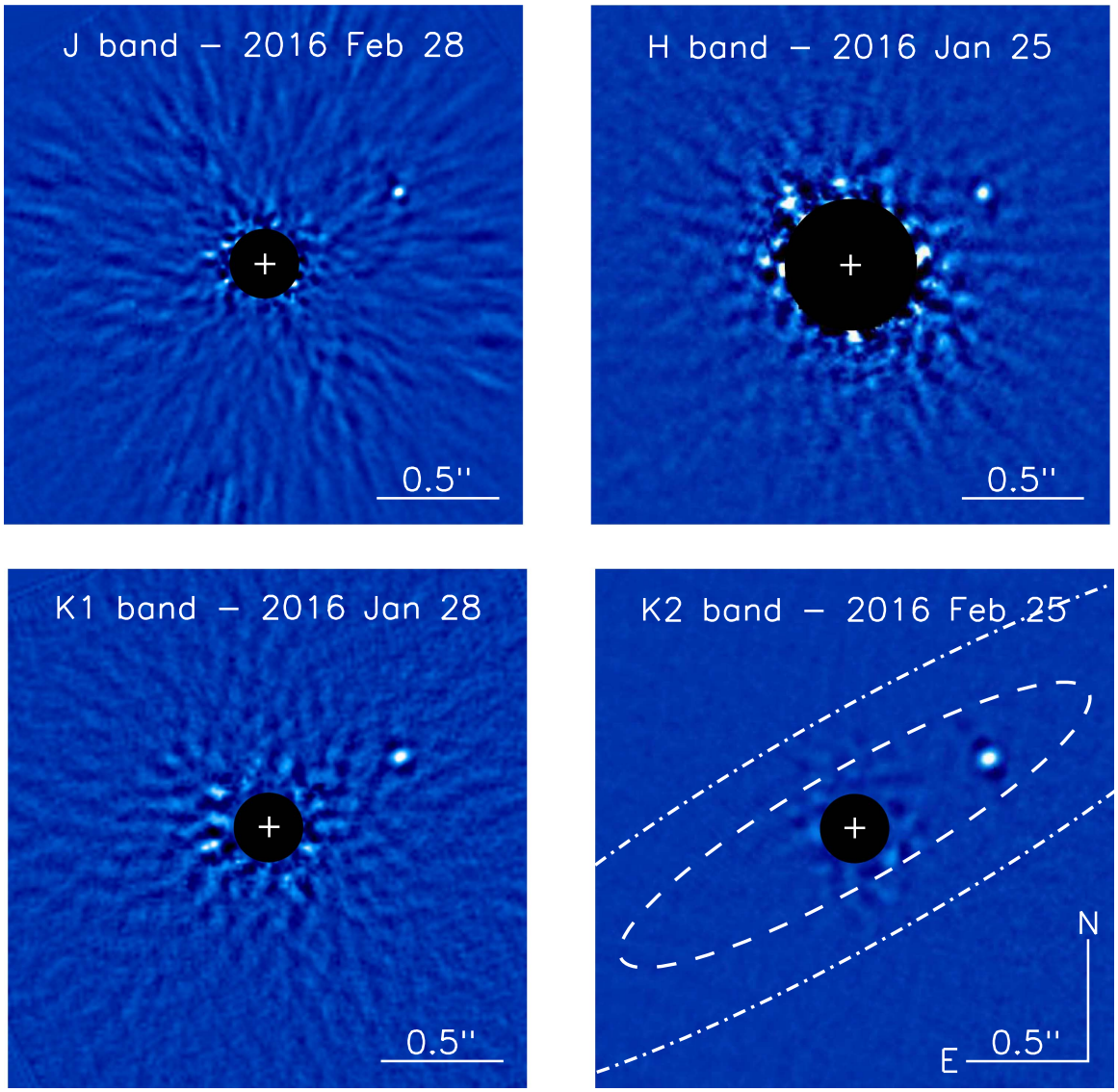

Figure 1. Collapsed datacubes showing HR 2562B in each of the four modes observed with GPI and reduced using KLIP. The *K*2 image is from 2016 February and demonstrates two possible solutions for the inner edge of the disk (38 and 75 au are indicated with dashed and dot–dashed lines, respectively) assuming an inclination of 78° and a position angle of 120°.

described in Macintosh et al. (2015) and De Rosa et al. (2015), using four independent pipelines and several ADI algorithms: cADI (Marois et al. 2006), TLOCI (Marois et al. 2014), and KLIP/pyKLIP (Soummer et al. 2012; Wang et al. 2015). The post-processed cubes were then combined to create broadband images, examples of which are shown in Figure 1. From each of these pipelines, positions and contrast-per-slice and associated errors were extracted following the forward-modeled and minimization techniques described in Marois et al. (2010), Lagrange et al. (2010), and Pueyo (2016). The final astrometric errors were combined in quadrature from the errors on the measurements (0.20–0.35 px depending on the data set), astrometric calibration, and star center (0.05 px). For the spectroscopy, the errors on the measurements and on the star-to-spot ratio were similarly combined. Final values for astrometry and contrasts for the companion are derived by

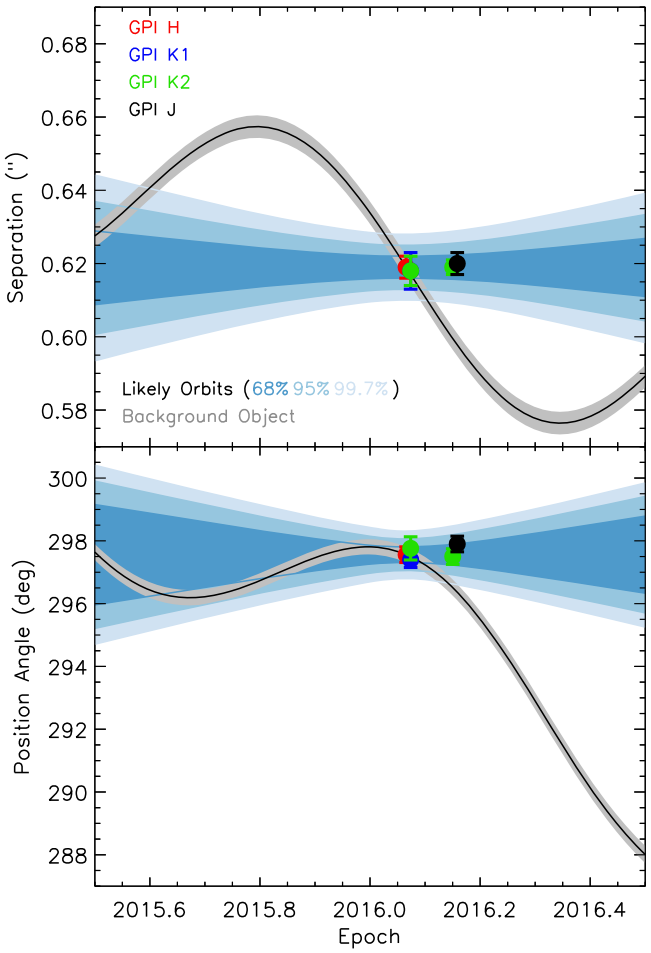

Figure 2. Astrometric data points for HR 2562B as a function of epoch. The gray lines show the path of a background object, while the blue shaded regions show the path of possible orbits for a bound companion.

averaging the results of each pipeline. Table 1 gives the astrometry and photometry derived from each observation set. The spectra of the companion were then obtained after normalization with a calibrated template F5V spectrum from the Pickles library (Pickles 1998), the 2MASS *JHK* magnitudes of the host star, and the GPI response functions. Figure 3 shows the final spectrum from each bandpass.

4. PROPERTIES OF HR 2562B

4.1. Companionship

At the distance of HR 2562, the projected separation of the companion is 20.3 ± 0.3 au ($0\farcs618 \pm 0\farcs003$). We assessed whether the candidate companion is comoving with the star. We compared all relative astrometric measurements with the predictions of the location of an infinitely far background object. The companion being an infinitely far background object is ruled out to 5σ (Nielsen et al. 2013). Additionally, following De Rosa et al. (2015), we estimate likely orbit tracks for bound objects. The results of this assessment are shown in Figure 2. The astrometry falls clearly in the realm of bound orbits, with a preferred range of semimajor axes of ~15–42 au.

Archival *Hubble Space Telescope* NICMOS data from 2007 were found for HR 2562 (PI: Rhee, ID 11157). These data were processed as part of the Archival Legacy Investigation of Circumstellar Debris Disks (ALICE; Choquet et al. 2014). Although the contrast achieved in these images is insufficient to detect the companion at its present location, we searched for point sources at the location the companion would have been if it were a background object ($\sim 1\farcs3$). No source is detected at this location.

As we demonstrate in Section 4.2, the companion photometry and spectroscopy are inconsistent with an infinitely far background star. A more likely source of contamination might instead be a non-stationary foreground or slightly background L/T dwarf. Following the methodology in Macintosh et al. (2015), we determine the probability of finding a L5-T5 type object in the GPI field of view by combining L and T dwarf space densities[36] and absolute magnitudes (Reylé et al. 2010; Pecaut & Mamajek 2013). We calculate a false alarm probability of 7×10^{-7} within the GPI field of view for L5-T5 dwarfs. Since the companion was found after observing 203 targets, the final false alarm probability is 1.4×10^{-4}. Therefore, the chance alignment of a non-stationary, unbound brown dwarf is unlikely and the bound status is more probable.

4.2. Spectral Comparisons to HR 2562B

Photometric and spectral comparisons were made to assess the likely properties of HR 2562B. First, we used several libraries of spectra and routines to determine the best-matching spectral type for HR 2562B. We used the SPLAT toolkit, which makes use of the SpeX prism library, to determine which spectral types match HR 2562B (Burgasser 2014). We find that the best-matching source comparing all three spectral bands simultaneously is WISE J174102.78-464225.5 (WISE 1741-4642), a recently discovered peculiar L7 $\pm$ 2 type brown dwarf with an estimated age of 10–100 Myr (Schneider et al. 2014). Classifying the HR 2562B using spectral standards in SPLAT returns a spectral type of L7 $\pm$ 0.5.

In a separate analysis, we used a χ^2 goodness of fit test with data from the SpeX Prism Library supplemented by spectra from Filippazzo et al. (2015). The χ^2 fits were produced by normalizing the empirical spectra to HR 2562B with a constant based on the flux and uncertainties of both spectra, following Cushing et al. (2008). The χ^2 values were then calculated between the empirical spectrum and HR 2562B and assessed as a function of spectral type. In this analysis, we considered all three bands simultaneously and separate fits to each of the bands individually. We find that sources with spectral types between L3.5 and T2 provide the best fits to the data, depending on the band. The best fit to the *J*-band is a T2 type object, while L3.5 and L4.5 sources best match *H* and *K*, respectively. The simultaneous fit to all bands returns the same best fit as SPLAT, WISE 1741–4642.

In our analysis of χ^2 as a function of spectral type, we find that while earlier spectral types are preferred at *H* and *K*, mid-to-late L types have nearly equivalent χ^2. We also find that two other young L/T transition objects, VHS J125601.92–125723.9B (VHS 1256B, Gauza et al. 2015) and PSO J318.5338-22.8603 (PSO 318, Liu et al. 2013), are reasonable matches to the spectra in individual bands. When considering the bands simultaneously, it is clear that the overall flux in each wavelength is not perfectly matched by any other object, including the best-fit WISE 1741–4642. However,

[36] We assume a uniform space density of brown dwarfs, given that our observations could only detect L5-T5 objects at less than the scale height of the thin disk.

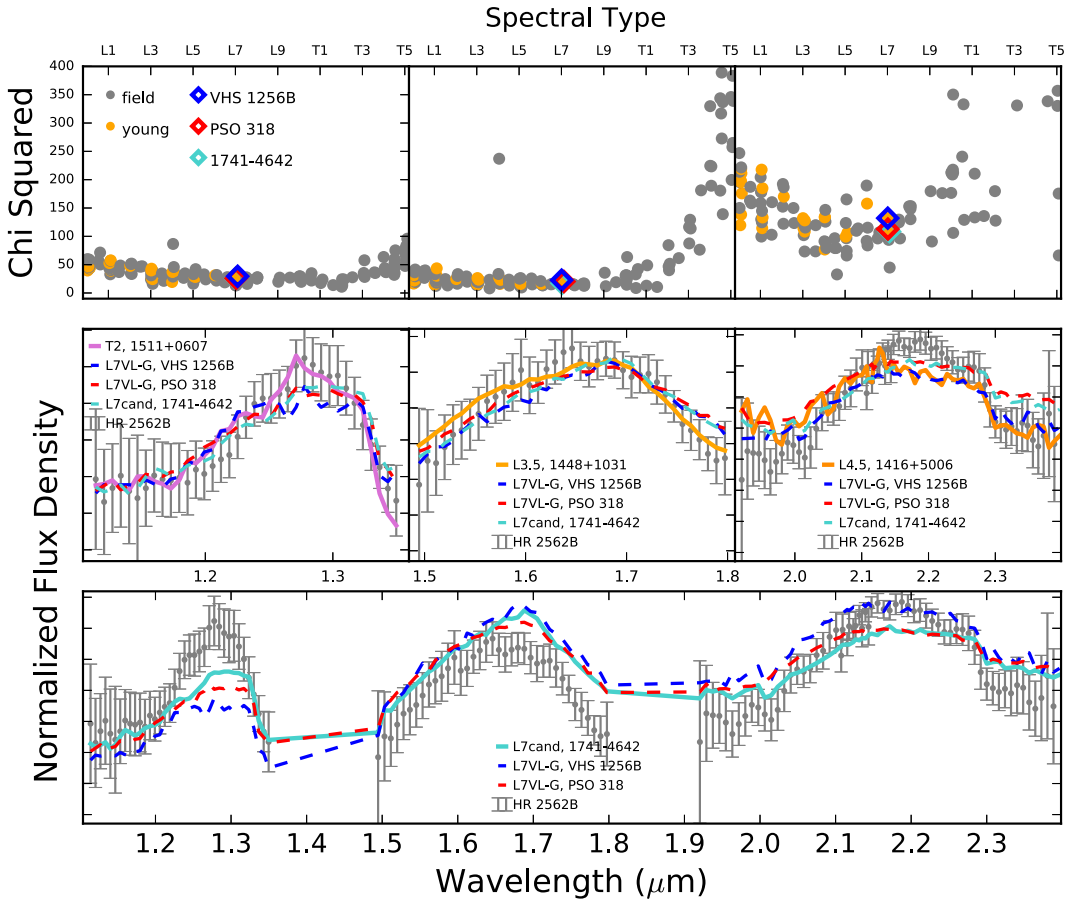

Figure 3. The spectrum of HR 2562B (gray) shown with the best-fitting objects (solid lines) per band (middle row), and the best fit (solid aqua line, WISE J1741-4642) across all bands (bottom row). Also shown are the young objects VHS 1256B and PSO 318 (dashed blue and red lines), which are both reasonable matches to the spectra. The corresponding χ^2 as a function of spectral type is plotted for each band (top row).

(The data used to create this figure are available.)

brown dwarfs can have similar spectral features despite varying flux in different wavelength bands (i.e., a range of colors), as shown, for example, by Leggett et al. (2003) and Cruz et al. (2016). To investigate this, Cruz et al. (2016) created band-normalized templates from optically classified field L0-L8 and L0γ–L4γ objects and found that objects with a range of $J-K$ colors as large as 0.60 can match band-normalized templates with an average $\chi^2 > 0.9$. We therefore adopt a spectral type of L7 $\pm$ 3 for HR 2562B. Figure 3 shows the spectrum of HR 2562B, along with the spectra of the best-fitting objects in each band and other similar young objects.

We then compare the colors of HR 2562B with other objects in color–magnitude diagrams (see Figure 4). The source clusters with the sequence of young, red, L-type objects in the M_J versus $J-K$ and M_H versus $H-K$ diagrams. Its $H-K$ is similar to VHS 1256b and PSO 318. It is somewhat bluer in $J-K$, though it is still near PSO 318 in absolute magnitude at M_J. Its consistency with young L-type objects is an additional suggestion of youth (e.g., Gagné et al. 2015).

We can also compare absolute photometry to other brown dwarfs in both the field and young moving groups. The variation of the J-band magnitude with spectral type has been commonly used as a method of distinguishing between field and potentially young objects (e.g., Faherty et al. 2012), with younger L-type objects tending to be fainter at the J-band than older objects of the same spectral type. This is thought to be a natural consequence of changes in surface gravity with age impacting atmospheric properties such as clouds (e.g., Marley et al. 2012). Figure 4 shows the J-band magnitude variation with spectral type. At a spectral type of L7, HR 2562B clusters strongly with members of nearby moving groups below the field population.

Following the methods of Filippazzo et al. (2015), we constructed a spectral energy distribution (SED) using the spectra and photometry to determine an empirical $\log(L_{\rm bol}/L_\odot)$ of -4.62 ± 0.12. Using this value and an age range of 300–900 Myr, we then use the evolutionary models from Saumon & Marley (2008) to estimate the physical properties of HR 2562B (solar metallicity, hybrid cloud). We find a mass of 30 $\pm$ 15 $M_{\rm Jup}$, a radius of 1.11 $\pm$ 0.11 $R_{\rm Jup}$, a $\log(g)$ of 4.70 $\pm$ 0.32, and a temperature of 1200 $\pm$ 100 K. This temperature is somewhat lower than field L7 type objects, but is consistent with estimates for young objects of this spectral type.

5. HR 2562B AND THE DEBRIS DISK

The identification of a brown dwarf in a system with a debris disk presents interesting opportunities for constraining system properties. In *Herschel* PACS images, the disk is marginally resolved. Moór et al. (2015) use this data to derive an average dust radius of 112.1 $\pm$ 8.4 au, with evidence for an inner hole of radius between ~18–70 au. The average outer radius is found to be 187 au. Interestingly, they find that the disk has a

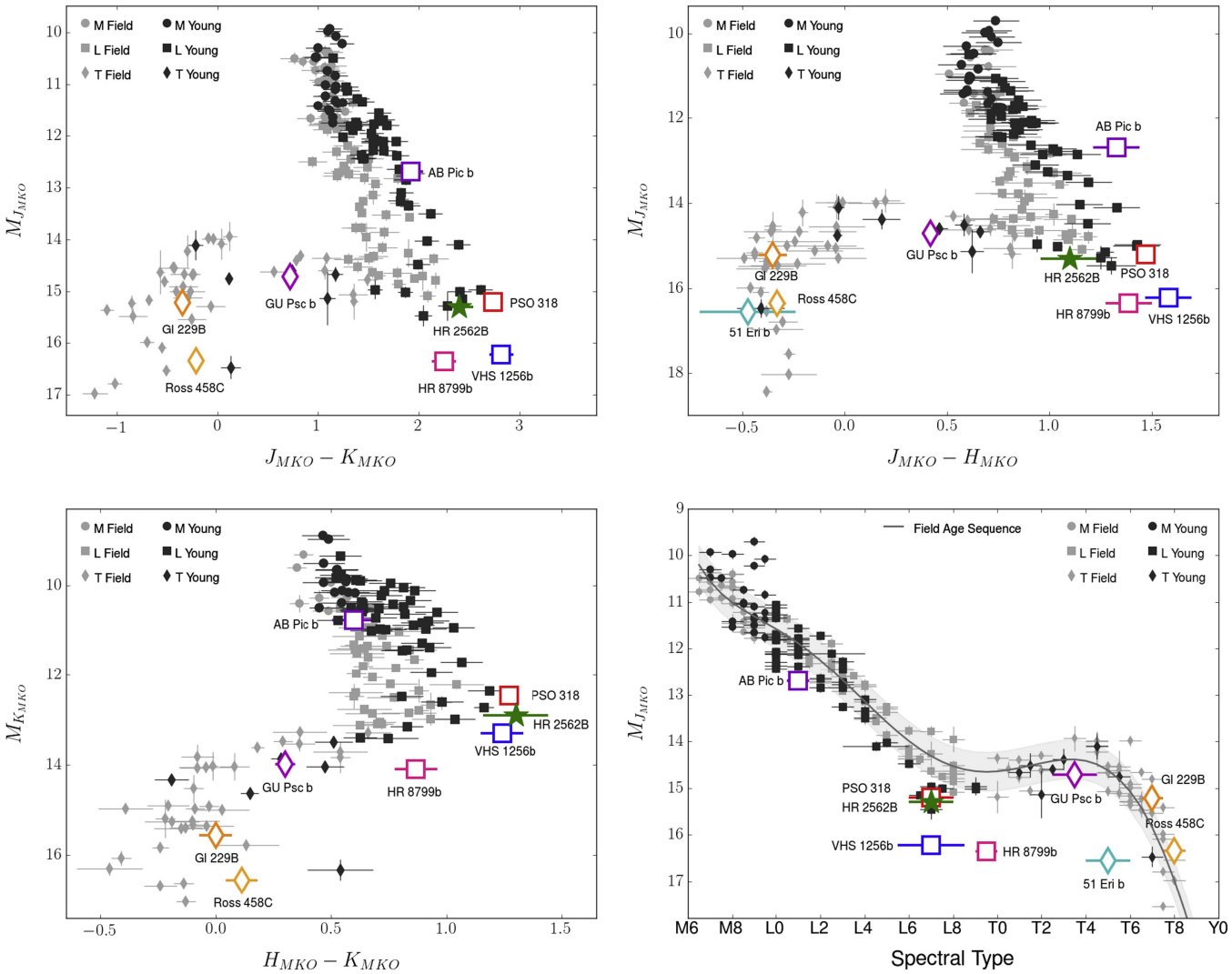

Figure 4. Top row and bottom left: color–magnitude diagrams (*JHK*) with the MLT sequence of 180 field objects (light gray symbols) from Filippazzo et al. (2015). Young brown dwarfs or directly imaged companions are also shown (black symbols), and a few peculiar objects (specific symbols) from Best et al. (2015), Faherty et al. (2016), and J. Gagné et al. (2016, in preparation). Bottom right: the *J*-band absolute magnitude as a function of spectral type. The gray line shows the field sequence with the 1σ spread marked by the gray shaded area following Filippazzo et al. (2015).

high inclination of $78\overset{\circ}{.}0 \pm 6\overset{\circ}{.}3$ and a position angle on the sky of $120\overset{\circ}{.}1 \pm 3\overset{\circ}{.}2$. Given the separation of HR 2562B of ~20 au and an average position angle of ~298°, the source appears to be interior to the hole in the disk and coplanar with the disk to within the uncertainties (see Figure 1). This is the first example of a brown dwarf-mass companion within the inner hole of a debris disk.

The existence of a companion interior to the disk provides the exciting possibility of independently constraining the properties of the HR 2562 system. Moór et al. (2015) discuss the possibility of a self-stirring mechanism generating the resolved disk material for a source as old as HR 2562A. In this mechanism, secular perturbations from a companion generate enhanced collisions of smaller planetesimals, leading to the generation of dust at wide separations (Mustill & Wyatt 2009). Using Equation (6) in Moór et al. (2015), and assuming their nominal disk parameters, we find that a mass of only $13 M_{\rm Jup}$ would be required to generate collisions out to ~187 au in 900 Myr, assuming an eccentricity of 0.01. If we use 30 $M_{\rm Jup}$ for HR 2562B, we derive a crossing time of ~385 Myr, consistent with the lower end of our adopted age range. While the uncertainties in the outer radius of the disk and mass of the planet allow for crossing times of >1 Gyr, the nominal parameters are consistent with the scenario that HR 2562B is responsible for generating the observed disk.

A more complicated question is whether the inner hole can also be used to place an upper limit on the mass of the companion. Though Moór et al. (2015) derive an average inner radius of 38 ± 20 au from *Herschel* images, the uncertainty on this value is fairly large. Moór et al. (2015) also performed a separate SED fit to available photometry and derived an inner radius of 64 ± 6 au. Since these two values are not consistent, we performed a quick analysis in which we simultaneously fit the SED and the *Herschel* PACS image using MCFOST (Pinte et al. 2006). We used the geometric parameters from Moór et al. (2015), a flat surface density profile, and a minimum grain size of about 1 micron. We find that the SED and image together are best reproduced using an inner radius of ~75 au. This radius is consistent with the upper end of the uncertainty range and SED fit of Moór et al. (2015). For completeness, we use both an inner radius of 38 au and our derived value of 75 au to roughly determine whether mass constraints are possible.

Using the dynamical stability criterion proposed by Petrovich (2015), we estimate the mass of the HR 2562B, assuming

it is responsible for clearing the inner hole and that it has an eccentricity of zero. We find that if the inner hole is 38 au, the upper limit on the mass of the companion is ~20 $M_{\rm Jup}$. The difference between an age of 300 and 900 Myr is negligible given our other assumptions. If instead we use an inner radius of 75 au, the upper limit on the mass is ~0.24 $M_{\odot}$, well beyond the highest estimates from evolutionary models. If the inner radius is indeed >75 au, it might suggest an elevated eccentricity for HR 2562B. Future observations that constrain the orbital parameters of the companion and high-resolution images of the disk will offer insight into the potential history of interaction between the bodies in this system and provide meaningful mass limits.

6. CONCLUSIONS

The HR 2562 system offers a relatively rare opportunity to probe the direct dynamical interaction of a substellar object with a Kuiper Belt analog. The overall system architecture may provide interesting clues to the formation of the companion. With a mass ratio of $q = 0.02 \pm 0.01$, HR 2562B is a new object in the growing list of substellar companions within 30 au (e.g., Hinkley et al. 2015; Mawet et al. 2015). These are excellent candidates for formation via disk instability, which has been shown to naturally produce objects as massive as 42 $M_{\rm Jup}$ at separations $\gtrsim$70–100 au (e.g., Rafikov 2005; Kratter et al. 2010). Several challenges to this picture remain, however, particularly the proximity of observed objects to their host stars. At such close separations the fast cooling needed for the disk fragmentation into bound objects becomes difficult to realize, precluding in situ formation of these brown dwarfs by gravitational instability (e.g., Rafikov 2005). However, it is plausible that the relatively massive HR 2562B formed beyond 50–70 au and migrated inward to its current location (e.g., Vorobyov 2013). Constraining the true mass and orbit of the companion is essential for determining its possible origin, which could offer evidence of planet formation above the deuterium burning limit.

The authors thank Richard Gray for his clarifying points on spectral classification. We also thank Adam Burgasser and Daniella Bardalez-Gagliuffi for helpful discussions. We also thank the anonymous referee whose comments improved this manuscript. This research has benefited from the SpeX Prism Library and SpeX Prism Library Analysis Toolkit, maintained by Adam Burgasser at http://www.browndwarfs.org/spexprism, from the BANYAN II web tool at http://www.astro.umontreal.ca/gagne/banyanII.php?targetname=HR+2562&resolve=Resolve, and from the SIMBAD database, operated at CDS, Strasbourg, France. This work is based on observations obtained at the Gemini Observatory, which is operated by the Association of Universities for Research in Astronomy, Inc., under a cooperative agreement with the National Science Foundation (NSF) on behalf of the Gemini partnership: the NSF (United States), the National Research Council (Canada), CONICYT (Chile), the australian Research Council (australia), Ministério da Ciência, Tecnologia e Inovação (Brazil) and Ministerio de Ciencia, Tecnología e Innovación Productiva (Argentina). J.R., R.D. and D.L. acknowledge support from the Fonds de Recherche du Québec. This work was supported by NSF grants AST-1518332 (R.J.D.R., J.R.G., J.J.W., T.M.E., P.K)., AST-1411868 (B.M., A.R., K.W.D.), AST-141378 (G.D.), AST-1211568 (P.A.G., E.L.R.), DGE-1232825 (A.Z.G.), and AST-1313132 (J.F.C., E.L.R.). This work was supported by NASA grants NNX15AD95G/NEXSS and NNX15AC89G (R.J.D.R., J.R.G., P.K., J.J.W., T.M.E.), and NNX14AJ80G (E.L.N., S.C.B., B.M., F.M., M.P.). Portions of this work were performed under the auspices of the U.S. Department of Energy by the Lawrence Livermore National Laboratory under Contract DE-AC52-07NA27344 (S.M.A., L.P., D.P.).

REFERENCES

Asiain, R., Figueras, F., Torra, J., & Chen, B. 1999, A&A, 341, 427
Bate, M. R. 2012, MNRAS, 419, 3115
Best, W. M. J., Liu, M. C., Magnier, E. A., et al. 2015, ApJ, 814, 118
Burgasser, A. J. 2014, ASInC, 11, 7
Casagrande, L., Schönrich, R., Asplund, M., et al. 2011, A&A, 530, A138
Choquet, É., Pueyo, L., & Hagan, J. B. 2014, Proc. SPIE, 9143, 914357
Cruz, K. L., Núñez, A., Burgasser, A. J., et al. 2016, ApJS, submitted
Cushing, M. C., Marley, M. S., Saumon, D., et al. 2008, ApJ, 678, 1372
De Rosa, R. J., Nielsen, E. L., Blunt, S. C., et al. 2015, ApJL, 814, L3
Faherty, J. K., Burgasser, A. J., Walter, F. M., et al. 2012, ApJ, 752, 56
Faherty, J. K., Riedel, A. R., Cruz, K. L., et al. 2016, ApJS, 225, 10
Filippazzo, J. C., Rice, E. L., Faherty, J., et al. 2015, ApJ, 810, 158
Fuhrmann, K., & Chini, R. 2015, ApJ, 806, 163
Gagné, J., Faherty, J. K., Cruz, K. L., et al. 2015, ApJS, 219, 33
Gagné, J., Lafrenière, D., Doyon, R., Malo, L., & Artigau, É. 2014, ApJ, 783, 121
Gauza, B., Béjar, V. J. S., Pérez-Garrido, A., et al. 2015, ApJ, 804, 96
Gray, R. O., Corbally, C. J., Garrison, R. F., et al. 2006, AJ, 132, 161
Hinkley, S., Kraus, A. L., Ireland, M. J., et al. 2015, ApJL, 806, L9
Konopacky, Q. M., Thomas, S. J., Macintosh, B. A., et al. 2014, Proc. SPIE, 9147, 914784
Kratter, K. M., Murray-Clay, R. A., & Youdin, A. N. 2010, ApJ, 710, 1375
Kraus, A. L., Ireland, M. J., Martinache, F., & Lloyd, J. P. 2008, ApJ, 679, 762
Kuzuhara, M., Tamura, M., Kudo, T., et al. 2013, ApJ, 774, 11
Lagrange, A.-M., Bonnefoy, M., Chauvin, G., et al. 2010, Sci, 329, 57
Leggett, S. K., Hawarden, T. G., Currie, M. J., et al. 2003, MNRAS, 345, 144
Liu, M. C., Magnier, E. A., Deacon, N. R., et al. 2013, ApJL, 777, L20
Macintosh, B., Graham, J. R., Barman, T., et al. 2015, Sci, 350, 64
Macintosh, B., Graham, J. R., Ingraham, P., et al. 2014, PNAS, 111, 12661
Maldonado, J., Eiroa, C., Villaver, E., Montesinos, B., & Mora, A. 2012, A&A, 541, A40
Malo, L., Doyon, R., Lafrenière, D., et al. 2013, ApJ, 762, 88
Marley, M. S., Saumon, D., Cushing, M., et al. 2012, ApJ, 754, 135
Marois, C., Correia, C., Galicher, R., et al. 2014, Proc. SPIE, 9148, 91480U
Marois, C., Lafrenière, D., Doyon, R., Macintosh, B., & Nadeau, D. 2006, ApJ, 641, 556
Marois, C., Macintosh, B., & Véran, J.-P. 2010, Proc. SPIE, 7736, 77361J
Mawet, D., David, T., Bottom, M., et al. 2015, ApJ, 811, 103
Moór, A., Ábrahám, P., Derekas, A., et al. 2006, ApJ, 644, 525
Moór, A., Kóspál, Á., Ábrahám, P., et al. 2015, MNRAS, 447, 577
Mustill, A. J., & Wyatt, M. C. 2009, MNRAS, 399, 1403
Nielsen, E. L., Liu, M. C., Wahhaj, Z., et al. 2013, ApJ, 776, 4
Pace, G. 2013, A&A, 551, L8
Pecaut, M. J., & Mamajek, E. E. 2013, ApJS, 208, 9
Perrin, M. D., Ingraham, P., Follette, K. B., et al. 2016, Proc. SPIE, in press
Petrovich, C. 2015, ApJ, 808, 120
Pickles, A. J. 1998, PASP, 110, 863
Pinte, C., Ménard, F., Duchêne, G., & Bastien, P. 2006, A&A, 459, 797
Pueyo, L. 2016, ApJ, 824, 117
Rafikov, R. R. 2005, ApJL, 621, L69
Reylé, C., Delorme, P., Willott, C. J., et al. 2010, A&A, 522, A112
Rhee, J. H., Song, I., Zuckerman, B., & McElwain, M. 2007, ApJ, 660, 1556
Saumon, D., & Marley, M. S. 2008, ApJ, 689, 1327
Schneider, A. C., Cushing, M. C., Kirkpatrick, J. D., et al. 2014, AJ, 147, 34
Soummer, R., Pueyo, L., & Larkin, J. 2012, ApJL, 755, L28
Torres, C. A. O., da Silva, L., Quast, G. R., de la Reza, R., & Jilinski, E. 2000, AJ, 120, 1410
van Leeuwen, F. 2007, A&A, 474, 653
Vorobyov, E. I. 2013, A&A, 552, A129
Wang, J. J., Ruffio, J.-B., De Rosa, R. J., et al. 2015, pyKLIP: PSF Subtraction for Exoplanets and Disks, Astrophysics Source Code Library, ascl:1506.001
Wyatt, M. C. 2008, ARA&A, 46, 339